Research Square

Preprints are preliminary reports that have not undergone peer review.
They should not be considered conclusive, used to inform clinical practice,
or referenced by the media as validated information.

Can the tunnel magnetoresistance properties of ferritin in avian hair cell organelles generate neural signals like those that cause motion sickness in humans?

Christopher Rourk

crourk@jw.com

Citizen scientist

Research Article

Keywords: Calcium signaling, Cuticulosome, Ferritin, Hair cell, Iron release, Magnetoreception, Motion sickness, Tunnel magnetoresistance

Posted Date: November 25th, 2026

DOI: https://doi.org/10.21203/rs.3.rs-11682249/v1

License: This work is licensed under a Creative Commons Attribution 4.0 International License.
Read Full License

Additional Declarations: No competing interests reported.

Can the tunnel magnetoresistance properties of ferritin in avian hair cell organelles generate neural signals like those that cause motion sickness in humans?

Chris Rourk[a,*]

[a] Citizen scientist, formerly with U.S. Nuclear Regulatory Commission, Office of Nuclear Regulatory Research

[*] Corresponding author: Chris Rourk, P.O. Box 670052, Dallas, TX United States 75367. crourk@jw.com. Telephone: 469-556-3482.

Abstract

Cuticulosomes are iron-rich organelles in the cuticular plate of avian hair cells that contain tens of thousands of ferritin-like granules, frequently arranged in highly ordered linear arrays. More than a decade after their discovery, no explanation has been established for their function. Recent studies have shown that ferritin supports long-range electron transport, exhibits tunnel magnetoresistance of 25 ± 5% at room temperature, and releases Fe^{2+} nonlinearly as electrons accumulate in its core, while other studies have shown that intracellular iron can trigger calcium signaling through redox-sensitive ryanodine receptors. Drawing on these findings, this paper proposes the hypothesis that the ordered ferritin arrays of cuticulosomes use the tunnel magnetoresistive properties of ferritin to redistribute electrons under the Lorentz force generated by movement through the geomagnetic field, causing iron release from ferritin particles at the edge of the array and contributing to hair cell calcium signaling. Because the Lorentz force on an electron or polaron is greatest when the velocity vector is orthogonal to the geomagnetic field and

absent when the two are parallel, the mechanism predicts significantly more signaling during east–west travel than during north–south travel. Order-of-magnitude estimates indicate that iron release from a single cochlear cuticulosome could reach approximately 49 μM in a 1 pL cytoplasmic volume, exceeding reported thresholds for calcium signaling in astrocytes and neurons. The resulting signals could resemble the hair cell signals that can trigger motion sickness in humans due to mismatch between visual cues, physical/vestibular cues (from the inner ear), and proprioceptive signals (from muscles and joints), and could discourage east–west travel. Ten experiments are proposed to test the hypothesis.

Keywords: Calcium signaling; Cuticulosome; Ferritin; Hair cell; Iron release; Magnetoreception; Motion sickness; Tunnel magnetoresistance

1. Introduction

In 2013, an iron-rich organelle in the cuticular plate of avian hair cells, the cuticulosome, was reported (Lauwers et al., 2013). The iron was determined to be stored in ferritin, an iron storage protein complex found in most living cells that includes a protein shell that self-assembles from light-chain and heavy-chain protein subunits. In cuticulosomes, the heavy-chain components predominate, which are useful for quickly storing Fe2+ (Nimpf et al. 2017). This structure suggests that cuticulosomes frequently handle cytosolic Fe2+ transients. Ferritin is an important component of the labile (free or Fe^{2+}) iron pool (LIP), a cell-specific collection of proteins and enzymes that tightly regulates labile iron to prevent it from interacting with hydrogen peroxide in Fenton's reaction to generate damaging reactive oxygen species (ROS) (Kakhlon and Cabantchik, 2002). The core of ferritin primarily contains iron oxides in the form of ferrihydrite, but can contain other elements such as phosphorus. An example of a cuticulosome is shown in Fig. 1.

While Nimpf et al. (2017) characterized these structures as paracrystalline arrays, that is not correct. Paracrystalline generally denotes short to medium range order, whereas crystalline generally denotes long-range order (Bregado et al., 2019). The highly linear arrays present in many cuticulosomes exhibit long distance order and would be more properly characterized as crystalline, but even that characterization could be misleading if the physical mechanism that is imposing the order is assumed to be due to ionic bonds as opposed to magnetic, electrostatic or other physical mechanisms. It would be improper to assume that these are merely textbook examples of polycrystalline colloidal crystallization. It would also be a mistake to assume that these unusual organelles are merely associated with the functions of the labile iron pool, which all other cells accomplish without such unusual organelles. Further research is needed to understand what these organelles are, how they function and why they have such unusual ferritin structures.

Cuticulosomes average about 545 nm in diameter in cochlear hair cells and about 365 nm in vestibular hair cells, and consist of ferritin-like granules having electron-dense cores of about 6.5–6.75 nm in diameter, sometimes in highly ordered arrays and where the dominant core material is ferrihydrite. The organelle contains tens of thousands of ferritin-like granules and tests positive for ferritin heavy chain ferritin by immunostaining. The magnetically responsive neurons in the pigeon vestibular nuclei depend on an intact cochlear duct, placing the cuticulosome of the pigeon (*Columba livia*) in tissue implicated in magnetic sensing. One study has proposed that cuticulosomes may regulate inner-ear ionic conditions and thereby indirectly tune a magnetic sensor based on electromagnetic induction, which is one of three candidate mechanisms for magnetoreception that have been previously identified in the literature and studied in detail without success at demonstrating a link to magnetosensation (de Gille et al., 2021).

The objective of this paper is to evaluate whether the known biophysical properties of ferritin could allow the ordered ferritin arrays of cuticulosomes to transduce the geomagnetic field into iron release and calcium signaling, to estimate whether the magnitude of such iron release is physiologically plausible, and to propose experiments that could test the resulting hypothesis.

2. Materials and methods

This study is a theoretical analysis that develops and evaluates a testable hypothesis. No new animal experiments or field work were conducted; all data used were taken from previously published studies, which are cited where used.

2.1. Literature synthesis

Published experimental findings were assembled on (1) the structure and composition of cuticulosomes in avian hair cells; (2) the electron transport, tunnel magnetoresistance, and spin-filtering properties of ferritin and of comparable man-made nanostructures, including iron oxide nanoparticles and quantum dots; (3) the electron storage and iron release behavior of ferritin; (4) the relationship between intracellular iron, reactive oxygen species, and calcium signaling in neurons and astrocytes; and (5) the association of ferritin-rich cells with magnetosensation in other animals. Results of these studies are summarized in Section 3.

2.2. Order-of-magnitude calculations

The force on an electron moving through the geomagnetic field was estimated from the Lorentz force equation (Eq. (1)), using a velocity of 10 m/s and geomagnetic field strengths of approximately 24–60 μT. The distance that such a force could move a free electron over the ~400 μs lifetime of a trap state reported for ferrihydrite nanoparticles (Soltis et al., 2017) was calculated from classical kinematics. The number of ferritin particles in a cuticulosome was estimated from

the reported cuticulosome diameters of ~545 nm (cochlear) and ~365 nm (vestibular), assuming that each identified particle is a ferritin particle and a packing fraction of 0.7. Iron release was estimated from the in vitro measurements of Watt et al. (1985), assuming an Fe^{3+} content of 2,300 ions per ferritin particle, a release of 450 Fe^{2+} ions per ferritin particle, and a hair cell cytoplasmic volume of about 1 pL (1,000 μm^3). The resulting concentrations were compared with calcium-signaling benchmarks reported for astrocytes (Guan et al., 2021) and neurons (Muñoz et al., 2011).

2.3. Design of proposed tests

Experimental tests were designed so that each yields a prediction that differs depending on whether the hypothesis is correct, using behavioral, neural-activity, ablation, pharmacological, and tissue-marker endpoints (Section 4.1; Table 5).

3. Results

3.1. Ferritin exhibits quantum confinement and tunneling magnetoresistance properties similar to those of man-made materials

The highly ordered arrays of ferritin particles like those in cuticulosomes have been shown to be capable of long distance electron transport under the right circumstances (Bera et al. 2019; Rourk et al., 2021). Notably, this effect does not appear to be strongly influenced by the proportion on heavy chain or light chain components, as electron tunneling associated with ferritin is present in both archaeon ferritin that is predominantly heavy chain as well as horse spleen ferritin that is predominantly light chain (Kumar et al., 2016). Electron and proton transport through the protein shell of ferritin is required for oxidation of Fe^{2+} ions to Fe^{3+} ions and storing them as iron oxides. Light-chain subunits of the protein shell can conduct electrons into and out of the core, where the ferrihydrite can trap electrons, reducing Fe^{3+} to Fe^{2+}. Electrons and protons can be captured by the

protein shell and transferred to the mineral core, where electron transport is consistent with long-distance transfer, possibly by tunneling, through the 2.0–2.5 nm shell (Watt et al., 1985; Wolszczak and Gajda, 2010).

In addition, ferritin has unusual magnetic properties that go beyond that of the superparamagnetic iron oxide nanoparticles (SPION) that may form in the core. Ferritin tunnel junctions show tunnel magnetoresistance of 60 ± 10% at 200 K and 25 ± 5% at room temperature, whereas apoferritin (the iron-free form of ferritin) shows none, so the effect depends on the iron core (Karuppannan et al., 2021). Tunnel magnetoresistance devices are used in cell phones to detect micro Tesla level magnetic fields (Deak et al., 2017), which demonstrates that the tunnel magnetoresistance mechanism can detect the geomagnetic field. In addition, SPIONs surrounded by chiral molecules similar to the structure of ferritin have been demonstrated to exhibit ferromagnetic behavior, with remnant magnetic fields of 80 Oersteds (Koplovitz et al., 2019; Zhu et al., 2024), and ferromagnetic magnetite nanoparticle arrays have been shown to retain about 12% magnetoresistance at room temperature (Zeng et al., 2006). In ordered arrays of scatterers, the Lorentz force redirects current toward exits and along edges, illustrating how a magnetic field can steer electron flow through a periodic structure like that of ferritin particles in a cuticulosome (Zozoulenko et al., 1997). This evidence establishes that a feasible theoretical mechanism for electron transport exists that can explain the observed electron transport data from ferritin arrays.

Ferritin has other electric and magnetic properties that have not been considered in the earlier studies of ferritin in the field of avian magnetosensation. At low temperatures, ferritin can operate as a single-electron transistor, with electrons tunneling from an electrode into the core and out to a second electrode (Labra-Muñoz and van der Zant, 2024). At room temperature, electron tunneling through a layer of ferritin – a distance of approximately 12 nm - resulted in

approximately 1 electron tunneling event per ferritin core every 10 to 10^6 seconds across large numbers of ferritin particles in parallel between electrodes in a self-assembled monolayer, depending on the iron loading of the core (Kumar et al., 2016). In contrast, sequential electron tunneling in devices through thousands of adjacent ferritin particles deposited in multiple layers (Bera et al. 2019; Rourk et al. 2021) resulted in 10^6 to 10^8 electron tunneling events per second through individual particles ranging from (Table 1).

These data show that electron tunneling through arrays of ferritin occurs at rates that are significantly higher than electron tunneling through individual cores and at lower effective voltage differentials, which is generally consistent with studies of disordered arrays of quantum dots (Jha and Middleton, 2005) and the behavior of arrays of magnetic nanoparticles.

Karuppannan et al. (2021) provide experimental evidence of electron transport through ferritin in a direction that is orthogonal to an applied magnetic field vector. In its ferritin junctions, magnetoresistance was measured with an in-plane magnetic field, meaning a field parallel to the bottom nickel electrode. Electrons tunneled across the ferritin layer between the bottom and top electrodes. The current therefore ran roughly perpendicular to the field. In that geometry, the ferritin junctions showed tunnel magnetoresistance of 60 ± 10% at 200 K and 25 ± 5% at room temperature. Charge transport through iron-loaded ferritin did not depend on temperature, which points to long-range coherent tunneling rather than thermally activated hopping. The authors proposed that this tunneling is assisted by magnons, which are collective spin excitations in the magnetic nanoparticles inside the ferritin. Under that model, the field controls whether successive particles' anisotropy axes line up with the polarization of incoming electrons, and so modulates resistance. At about 1.0 T all particles were magnetically aligned, which favored magnon-assisted

transport through the junction, but magnetic alignment and hysteresis was observed even at substantially lower field levels. The resulting magnetoresistance curves are shown in Fig. 2.

These data indicate that the ferritin cores were spin-polarized and that the protein shell decoupled them magnetically from the nickel electrode. Each ferritin particle therefore acted as a spin filter. In this configuration, iron cannot leave the core, so the observed variability in physical properties would likely be due solely to electron dynamics in the core and through the protein shell and the interaction of each particle with other particles. These unusual physical properties of ferritin are also biophysical properties, and in cytoplasm or the environment with organelles such as cuticulosomes, there will be additional ion dynamics such as electrons, proton, Fe^{2+} ions and possibly other elements entering and leaving the core. It is noted that ferritin-rich structures such as oligodendrocyte precursor cells in the substantia nigra pars compacta provide endogenous magnetic resonance imaging contrast, indicative of aligned magnetic moments and other magnetic properties, although the reason for such high levels of ferritin in those tissues is still unknown (Hulet et al., 2000; Mangia et al., 2013).

Quantum dots (QDs) are man-made semiconductor devices that have electron confinement properties similar to those that have been demonstrated in ferritin. QD studies have also shown that a field perpendicular to the plane of transport shapes electron flow through dot structures. In a study of non-magnetic graphene QDs under a perpendicular field, conductance rose at low but increasing fields. The authors attributed this to reduced backscattering, with a peak near 1.5 T (Güttinger et al., 2011). At higher fields, magnetic confinement produced additional, strongly coupled localized dots. In a study of triangular triple QDs, a perpendicular magnetic field was used to engineer degeneracies in the energy levels that produced Aharonov–Bohm oscillations and current dips that repeated with each flux quantum or half flux quantum (Delgado and Hawrylak,

2008). The field therefore acted as a control on coherent transport through a small array of dots. A study of lateral QDs under a perpendicular magnetic field showed that spin-dependent tunneling caused spin blockade and negative differential conductance (Rogge et al., 2006). In a study that used topological insulator QDs, the magnetic field lifted spin degeneracy and produces spin-polarized current (Zhang et al., 2013). The authors suggested that the resulting spin splitting could be used as a spin filter. In a tight-binding QD model, a strong perpendicular magnetic field created edge states even in small dots (Moldoveanu et al., 2000). The edge states were stable against electron-electron interaction. And in studies of single-level QDs, applied magnetic fields produced a Zeeman effect that split the current steps and the Kondo-regime conductance features by the Zeeman energy (Yang et al., 2018; Zhuravel et al., 2019).

Applied to ferritin arrays, these findings suggest the following mechanism. Electrons moving through an array of ferritin cores orthogonal to a magnetic field could enter cores whose magnetic nanoparticles have been aligned by the field (Karuppannan et al., 2021), or transient ferromagnetic properties imparted by electron, proton and Fe2+ transport through the protein shell (Koplovitz et al., 2019; Zhu et al., 2024). The chiral shell and ferrihydrite-bearing core could spin-filter those electrons (Bera et al, 2019; Karuppannan et al., 2021; Rourk et al., 2021). Because the electrons' spin is matched to the aligned cores, magnon-assisted long-range tunneling from core to core would be favored (Karuppannan et al., 2021). That spin coherence, together with trapped electrons and polarons in the core, could extend tunneling across the array at room temperature (Soltis et al. 2017; Rourk et al., 2021). The QD studies further suggest that a magnetic field perpendicular to the direction of travel could produce spin-polarized current by lifting spin degeneracy (Zhang et al., 2013), raise conductance at moderate fields by reducing backscattering (Güttinger et al., 2011) and allow conductance to be tuned through interference effects in coupled dot arrays (Delgado and

Hawrylak, 2008). Accumulation of electrons in the cores of edge ferritin particles could lead to increased release of Fe2+ ions from the ferritin (Watt et al., 1985; Wolszczak and Gajda, 2010) and contribute to calcium signaling (Hidalgo and Núñez, 2007; Muñoz et al., 2011; Guan et al., 2021).

3.2. The function of hair cells in auditory structures

Given this extensive evidence of the ability of arrays of QDs to support electron transport, it is unlikely that ferritin with such a striking degree of order as that found in cuticulosomes could have evolved without a purpose in view of the unusual QD-like physical properties of ferritin, which implies a biophysical function. While these cuticulosomes have been extensively studied to see whether they could impart a mechanical force on the cell like a magnetically operated switch made by humans for electronics, that idea has been dismissed based on the evidence (Treiber et al., 2012; Malkemper et al., 2019).

It is also important to note that the LIP interacts with systemic iron levels. Recent tests demonstrated that depletion of macrophages with chlodronate resulted in the loss of magnetic sensation in homing pigeons (Lisowski et al. 2026). This would disrupt the storage and use of ferritin not only cuticulosomes and hair cells, but also in other cells (Koleini et al. 2021). It is important to understand the cellular and systemic processes that are used to handle iron in animals, because they are closely interrelated.

The location of the hair cells in the avian auditory structure is shown in Fig. 3. Hair cells are also found in pigeons extending from the crista ampullaris into the cupula in the semicircular canal, as shown in Fig. 4 (Nimpf et al., 2019). However, it is not known whether those hair cells contain cuticulosomes.

3.3. Generation of calcium signaling by iron release due to electron transport in ferritin

When humans experience seasickness/motion sickness, it is due to sensory conflict that involves movement of the fluid in the semicircular canal generating neural signals in the hair cells that do not correlate with other expected neural signals (Koch et al., 2018; Cohen et al., 2019). The cuticulosome of pigeons might not be present in locations where they can sense fluid movement in the semicircular canal, but based on other recent evidence (Mahmud et al., 2026), signals could possibly be generated by electron transport through ferritin causing iron release and associated calcium signaling (Rourk, 2025). This can be stimulated by east-west travel through the geomagnetic field, as shown in Fig. 5, in accordance with the Lorentz force equation:

$$\boldsymbol{F} = q(\boldsymbol{E} + \boldsymbol{v} \times \boldsymbol{B}) \qquad (1)$$

Earth's geomagnetic field is not uniformly horizontal or aligned exactly along a geographical north–south axis, and its inclination and declination vary with geographical location. While a pigeon travelling north–south would still experience a nonzero motional Lorentz force, particularly where the geomagnetic field has a substantial vertical component, all birds have to navigate in three dimensions against the wind, so their ability to sense and compensate for such variables would be well developed (Goto et al, 2017). If the pigeon is following other visual cues and the magnetic field effect is either expected or minor, then the visual cues would provide the dominant signal. How much iron release occurs as a function of inclination, how substantial the vertical component is, whether the vertical component is signaled differently from the other components and other variables will also likely be involved and need to be further investigated. The orientation of the arrays in the hair cells of the various macula could also be important for 3D sensation of the magnetic field. Further testing is needed to investigate these influences.

The component of the geomagnetic vector that is orthogonal to the velocity vector for birds traveling east or west can generate a force on free electrons in accordance with the Lorentz force equation, because the magnetic flux vector will generally be orthogonal to the velocity vector. That force could cause electrons to move through the ferritin arrays and crowd into ferritin particles at the end of the linear structures, resulting in release of iron, generation of ROS and the subsequent release of calcium from ryanodine receptors (RyR) and inositol trisphosphate receptors (IP_3R) in the endoplasmic reticulum (ER), which can result in calcium-induced calcium release (Hidalgo and Núñez, 2007; Muñoz et al., 2011; Guan et al., 2021). In contrast, the geomagnetic flux vector is parallel to the velocity vector for birds traveling north or south, which would result in no Lorentz force, no electron movement and no iron release.

For a free electron traveling in the geomagnetic field at a velocity of 10 m/s, the force would be approximately 4.0×10^{-23} to 1.0×10^{-22} N, which is useful as a figure of merit. It has been shown that ferritin can buffer electrons for hours in vitro, and there is also evidence that electrons are buffered in ferritin in vivo. In a ferrihydrite superparamagnetic iron oxide nanoparticle (SPION), electrons move through the crystalline iron oxide structures by polaronic hopping as small polarons, and can enter trap states for periods of up to ~400×10^{-6} s (Fig. 6).

A force of 4.0×10^{-23} N applied to an electron for 400×10^{-6} s will cause the electron to move ~3.5 meters. An electron in a trap state would not be able to persist while moving that distance, and would instead produce changes in the net charge of the semiconductor device (Morab et al., 2023). This figure of merit indicates that a significant amount of energy could be transferred to trap state electrons in ferrihydrite nanoparticles in the core of ferritin by interaction with the geomagnetic field. Electron dynamics for electrons in the core of ferritin have not been modelled using molecular dynamics and could also involve magnons, polarons and the Hall effect (Friedman and

Holstein, 1963; Cotleţ et al., 2019; Bao et al., 2023), but based on this rough analysis, it is at least possible that the Lorentz force could cause electrons stored in the cores of ferritin particles to move by inter-particle electron transport to ferritin particles on one side of the cuticulosome, where they could cause Fe^{2+} iron release into the cytoplasm. Regardless of the specifics of electron dynamics within the cores of individual ferritin particles, there is abundant evidence of room temperature electron tunneling and magnetoresistance effects that have been measured between iron oxide nanocrystals (Lekshmi et al., 2011), individual ferritin particles, and multilayer arrays of ferritin having a structure less ordered than the ferritin particles in cuticulosomes (Bera et al, 2019; Karuppannan et al., 2021; Rourk et al., 2021).

In a study of the electron storage and iron release behavior of ferritin, horse spleen ferritin containing 2,300 Fe^{3+} ions per particle was reduced anaerobically by loading electrons into the core with dithionite for 20 min and gel-filtered (Watt et al., 1985). At a loading of one electron per Fe^{3+} ion, the ferritin retained 1,850 Fe^{3+} ions, with a loss of 450 Fe^{2+} ions (about 20%) that was eluted as free Fe^{2+} ions. These release dynamics are summarized in Table 2.

These results indicate that low levels of electrons could be stored in the cores of ferritin throughout cuticulosomes under normal conditions, and could be transferred under the influence of the Lorentz force through tunnel magnetoresistance to result in high levels of electrons in the cores of edge ferritin particles in cuticulosomes, resulting in the release of Fe^{2+} ions into the cytoplasm and the generation of free radicals due to the interaction of Fe^{2+} ions and H_2O_2 in what is known as Fenton's reaction. The LIP quickly acts to regulate the levels of Fe^{2+} by storing the Fe^{2+} ions back into the ferritin cores. It is also unknown how the cuticulosome interacts with the LIP, and how the other contents of the cuticulosome interact with ferritin.

Studies have shown that iron entering hippocampal neurons enlarges the LIP and raises reactive oxygen species, including Fenton-derived hydroxyl radicals (Muñoz et al., 2011). These species promote calcium release through redox-sensitive ryanodine receptors. In one study, 20 μM iron produced ryanodine-sensitive calcium signals in neurons kept in calcium-free medium and activated extracellular signal-regulated kinases 1 and 2. Iron is required for sustained hippocampal long-term potentiation, and 20 μM $FeSO_4$ facilitated potentiation without altering baseline responses. In astrocytes, Fe^{2+} entering through divalent metal transporter 1 inhibits the Na^+/K^+-ATPase and reverses the Na^+/Ca^{2+} exchanger. Fe^{2+} and Fe^{3+} evoked calcium responses with an EC50 of about 0.4–0.6 μM, and signaling was activated above about 1 μM (Guan et al., 2021). Fe^{2+} ions can also enter neurons through calcium-permeable channels, including voltage-operated calcium channels and NMDA receptors (Codazzi et al., 2015). These studies all used extracellular iron to stimulate calcium signaling, but the structure of ferritin in cuticulosomes and the ability of ferritin to support inter-particle electron transport would allow Fe^{2+} ions to be released directly to the cytosol.

An order of magnitude estimate of the amount of Fe^{2+} release that would be required indicates that this hypothesis is feasible. The diameter of a cuticulosome is ~545 nm in the cochlea and ~365 nm in the vestibule. Assuming that each identified particle is a ferritin particle with a packing fraction of 0.7 yields ~66,000 ferritins per cochlear cuticulosome and about 20,000 per vestibular cuticulosome. Table 3 shows calculated release levels, assuming an Fe^{3+} ion content of 2,300 per ferritin particle and a release of 450 Fe^{2+} ions per ferritin particle, and a hair-cell cytoplasmic volume of about 1 pL (1,000 μm^3).

The amount of Fe^{2+} ions required to reach each calcium-signaling benchmark, assuming a 1 pL cytoplasmic volume, can be calculated based on the information reported in Guan et al. (2021) for astrocytes and in Muñoz et al. (2011) for neurons (Table 4).

On these assumptions, the levels of Fe^{2+} release observed by Watt et al. (1985) from a single cochlear cuticulosome could exceed every benchmark, remaining above 20 μM for cytoplasmic volumes up to about 2.4 pL. Reaching the astrocyte EC50 would require release of only about 5 Fe^{2+} per ferritin on the average. It is expected that the specific location and structure of the cellular compartment of the hair cell would have been optimized for this function by evolutionary processes, which could be further investigated using standard analytical techniques. It is noted that genetic ablation of the ferritin light-chain in the cochlear hair cells of mice results in alteration of calcium currents in those cells, indicative of a functional relationship between iron and calcium signaling in those hair cells (Petit et al., 2026).

3.4. Ferritin and magnetosensation in other animals

A non-exhaustive evaluation of ferritin's relationship to magnetosensation in other animals provides further observations that are relevant to the analysis of whether magnetic fields could contribute to iron release from ferritin and calcium signaling.

3.4.1. Rats

Evidence establishes that rats can avoid high magnetic fields, depending on an intact vestibular system. One important component of the vestibular system with elevated levels of ferritin are olfactory ensheathing cells (OECs) (Liu et al., 2024). OECs are phagocytes, a class of cells that include other types of cells with high levels of ferritin, such as macrophages (Soares and Hamza, 2016), glial cells, astrocytes, oligodendrocytes (Reinert et al., 2019) and Schwann cells (Mietto et

al., 2021). Ferritin-rich macrophages have also been identified as part of avian magnetosensory structures in the beaks of some types of birds (Treiber et al., 2012). Macrophages are also magnetically responsive and can change phenotype from M1 to M2 in response to exposure to magnetic fields (Wosik et al., 2018). As such, OECs are part of a closely related class of cell that have elevated levels of ferritin and that have been experimentally associated with magnetic sensation, and could be part of the magnetosensory system of rats. Calcium signaling in olfactory neurons is common from lower vertebrates to mammals (Takeuchi, 2024).

Examination of ferritin in the spleen of rats using magnetic force microscopy shows that it forms disordered arrays in organelles that are at best paracrystalline but which lack the linear arrays found in cuticulosomes (Blissett et al., 2017). The ferritin was identified in specimens that were prepared using a microtome from these organelles, and also appeared to have a remnant magnetization that is not characteristic of superparamagnetic iron oxide nanoparticles. This further evidence that electron transport could be occurring in those organelles and could be imparting ferromagnetic properties on the ferritin in those arrays.

3.4.2. Dogs

Evidence also establishes that dogs are sensitive to small variations of the Earth's magnetic field (Hart et al., 2013). As with rats, the extensive vestibular system of dogs also contains OECs (Gębarowski et al., 2025).

3.4.3. Fish

Sharks and other non-teleost fishes, such as skates, rays, sturgeons, paddlefishes, lungfishes, coelacanths and others have specialized sensory organs known as the Ampullae of Lorenzini that can detect electric fields (Newton et al., 2019). While the Ampullae of Lorenzini have substantial accumulations of electron dense material in the gel of ampullary canals, adjacent to the

endoplasmic reticulum (Whitehead et al., 2015), proteomic analyses of that gel to date have not identified the presence of ferritin (Zhang et al., 2018). In contrast, many fish, sharks and non-teleost fishes have an olfactory rosette (Hara, 1975) that contains olfactory ensheathing cells (Lazzari et al., 2013). The olfactory rosette has been associated with magnetosensory capabilities of some fish, such as salmon (Walker et al., 1997), but while it is also present in zebrafish (Lazzari et al., 2014), magnetite particles have also been found in the olfactory organ of zebrafish (Kirschvink et al., 2011). Because the relationship between ferritin and calcium signaling has not been investigated, further research is needed to determine whether that mechanism is present in the Ampullae of Lorenzini or olfactory rosette, as well as whether other signaling mechanisms can be deduced from observations such as the presence of magnetite or confirmed by testing.

3.4.4. Insects

The magnetic sensory organs of insects also contain abundant concentrations of ferritin (Keim et al., 2002; Wajnberg et al., 2018), and their neurons use calcium signaling (Hsu et al., 2007). For example, the chordotonal organs such as Johnston's Organ have been associated with magnetic sensory capabilities of insects (Jiang et al., 2024) and also use calcium signaling (Eatock, 2009).

4. Discussion

Birds must navigate in three dimensions against the wind, which places demands on their ability to navigate that animals limited to two dimensions do not have to contend with. Motion sickness in humans results from mismatch between visual cues physical/vestibular cues (from the inner ear), and proprioceptive signals (from muscles and joints). (Koch et al., 2018). In order to successfully navigate in three dimensions, birds must have acute awareness of unexpected changes in direction that are caused by the wind and the ability to closely track expected movements with

actual movements. While that is unlikely to result in the same exact experience that humans have when they suffer from motion sickness, that is possibly the closest human experience to the type of sensory experience that birds have when there is sensory mismatch between what they intend to do and what actually happens.

Dr. Joseph Bell, the Scottish surgeon who provided the inspiration for Sherlock Holmes, reportedly said "observe carefully, deduce shrewdly, and confirm with evidence." (Godbee, 1999) Because it is not possible to directly observe electron transport, the existence of it must be deduced from observations and confirmed with evidence of electron behavior that cannot be explained by classical mechanisms. It has been expressed by some who have studied magnetosensation that "it has to be cryptochrome" and that "the electromagnetic induction hypothesis is dead," (Nimpf and Keays, 2022), but those researchers were apparently unaware of the demonstrated relationship between iron and calcium signaling. For example, in response to the recent tests that demonstrated how systemic ferritin deficiency can impact magnetic sensation in homing pigeons, many experts were quick to criticize that work (Winklehofer and Hore, 2026; Kirschvink and Walcott, 2026), but failed to address 1) electron tunneling associated with ferritin, 2) the relationship between cytosolic iron and calcium signaling, 3) the effect that reduction in systemic ferritin would have on cellular ferritin levels or any of the other information discussed in this article, which has been known for decades. Ignoring important new information to promote entrenched ideas that fail to provide answers is unscientific. In light of the fact that ferritin is primarily an iron storage protein complex and not a mechanical switch, and in view of ferritin's unusual bioelectric and biomagnetic properties, perhaps the electromagnetic induction hypothesis should be revived. Dr. Bell noted in an interview in *The Pall Mall Gazette* published on December 28, 1893 that the failure to observe carefully, deduce shrewdly and confirm with evidence can lead to "a fatal mistake which the

ordinary policeman makes." Hopefully, the same will never be said about scientists investigating magnetosensation.

While the observations, deductions and evidence presented herein provide support for the hypothesis of an iron-calcium signaling mechanism that uses electron transport in ferritin, additional testing is needed to investigate that hypothesis. Because ferritin is a nanoscale biostructure, the direct observation of individual ferritin particles *in vivo* is likely not feasible, at least with present technology. However, the use of markers in combination with behavioral tests could lead to additional evidence to prove or disprove the hypothesis.

4.1. Proposed tests

A number of tests could be conducted to investigate this hypothesis. These are summarized in Table 5.

5. Conclusions

The geomagnetic field could potentially cause electron tunneling in ferritin particles due in part to the tunnel magnetoresistance of ferritin, similar to the devices used in cell phones to measure micro Tesla magnetic field transients. Electron transport in ferritin structures in cuticulosomes in pigeon hair cells could result in unexpected iron release and calcium signaling when the pigeons are traveling east or west, but not when they are traveling north or south. These signals could be similar to the signals that are generated when hair cells sense movement that creates a sensory conflict, making it possible that the sensation that is generated when birds travel east or west is similar to those that create motion sickness in humans, whereas no such sensation would be experienced when they travel north or south as intended. Thus, geomagnetic sensation would discourage unintended east or west travel, and would not discourage north or south travel.

Ethics statement

Not applicable. This study is a theoretical analysis based on previously published data, and no animal experiments or field work were conducted. Any of the experiments proposed in Table 5 would require prior approval from the appropriate institutional animal care and use committee and any required permits before being undertaken.

CRediT authorship contribution statement

Chris Rourk: Conceptualization, Formal analysis, Investigation, Methodology, Visualization, Writing – original draft, Writing – review & editing.

Funding

This research did not receive any specific grant from funding agencies in the public, commercial, or not-for-profit sectors.

Declaration of competing interest

The author declares that he has no known competing financial interests or personal relationships that could have appeared to influence the work reported in this paper.

Data availability

No new data were generated in this study. All data analyzed are available in the published sources cited.

Acknowledgments

References

Bao, S., et al., 2023. Direct observation of topological magnon polarons in a multiferroic material. Nat. Commun. 14, 6093.

Bera, S., et al., 2019. Long-range solid-state electron transport through ferritin multilayers. J. Mater. Chem. C 7, 9038–9048.

Blissett, A.R., et al., 2017. Magnetic mapping of iron in rodent spleen. Nanomedicine: NBM 13, 977–986.

Bregado, J.L., et al., 2019. Amorphous paracrystalline structures from native crystalline cellulose: a molecular dynamics protocol. Fluid Phase Equilib. 491, 56–76.

Codazzi, F., Pelizzoni, I., Zacchetti, D., Grohovaz, F., 2015. Iron entry in neurons and astrocytes: a link with synaptic activity. Front. Mol. Neurosci. 8, 18.

Cohen, B., et al., 2019. The neural basis of motion sickness. J. Neurophysiol. 121, 973–982.

Cotleţ, O., et al., 2019. Transport of neutral optical excitations using electric fields. Phys. Rev. X 9, 041019.

de Gille, R.W., et al., 2021. Quantum magnetic imaging of iron organelles within the pigeon cochlea. Proc. Natl. Acad. Sci. U.S.A. 118, e2112749118.

Deak, J.G., Zhou, Z., Shen, W., 2017. Tunneling magnetoresistance sensor with pT level 1/f magnetic noise. AIP Adv. 7(5).

Delgado, F., Hawrylak, P., 2008. Theory of electronic transport through a triple quantum dot in the presence of magnetic field. J. Phys.: Condens. Matter 20, 315207. https://doi.org/10.1088/0953-8984/20/31/315207

Eatock, R.A., 2009. Up, down, flying around. Nature 458, 156–157.

Friedman, L., Holstein, T., 1963. Studies of polaron motion: Part III: The Hall mobility of the small polaron. Ann. Phys. 21, 494–549.

Gębarowski, T., et al., 2025. Source-dependent phenotypic differences in canine olfactory ensheathing cell cultures from olfactory bulb and mucosa. Biomedicines 13, 3120.

Godbee, D.C., 1999. Joseph Bell (1837–1911): a clinician's literary legacy. J. Med. Biogr. 7, 166–170.

Goto, Yusuke, Ken Yoda, and Katsufumi Sato. "Asymmetry hidden in birds' tracks reveals wind, heading, and orientation ability over the ocean." *Science advances* 3.9 (2017): e1700097.

Guan, W., et al., 2021. Iron induces two distinct Ca^{2+} signalling cascades in astrocytes. Commun. Biol. 4, 525.

Güttinger, J., Stampfer, C., Frey, T., Ihn, T., Ensslin, K., 2011. Transport through a strongly coupled graphene quantum dot in perpendicular magnetic field. Nanoscale Res. Lett. 6, 253. https://doi.org/10.1186/1556-276X-6-253

Hara, T.J., 1975. Olfaction in fish. Prog. Neurobiol. 5, 271–335.

Hart, V., et al., 2013. Dogs are sensitive to small variations of the Earth's magnetic field. Front. Zool. 10, 80.

Hidalgo, C., Núñez, M.T., 2007. Calcium, iron and neuronal function. IUBMB Life 59, 280–285.

Hsu, C.-Y., et al., 2007. Magnetoreception system in honeybees (*Apis mellifera*). PLoS One 2, e395.

Hulet, S.W., et al., 2000. Oligodendrocyte progenitor cells internalize ferritin via clathrin-dependent receptor mediated endocytosis. J. Neurosci. Res. 61, 52–60.

Jha, S., Middleton, A.A., 2005. Effects of disorder on electron transport in arrays of quantum dots. arXiv preprint cond-mat/0511094.

Jiang, C., et al., 2024. Neuromorphic antennal sensory system. Nat. Commun. 15, 2109.

Kakhlon, O., Cabantchik, Z.I., 2002. The labile iron pool: characterization, measurement, and participation in cellular processes. Free Radic. Biol. Med. 33, 1037–1046.

Karuppannan, S.K., et al., 2021. Room-temperature tunnel magnetoresistance across biomolecular tunnel junctions based on ferritin. J. Phys.: Mater. 4, 035003.

Keim, C.N., et al., 2002. Ferritin in iron containing granules from the fat body of the honeybees *Apis mellifera* and *Scaptotrigona postica*. Micron 33, 53–59.

Kirschvink, J.L., et al., 2011. Magnetite-based magnetoreceptor cells in the olfactory organ of rainbow trout and zebrafish. AGU Fall Meeting Abstracts 2011.

Kirschvink, Joseph L., and Charles Walcott. "Quantitative reanalysis of classic pigeon homing experiments rejects a liver-based magnetic compass based on superparamagnetism." bioRxiv (2026): 2026-09.

Koch, Andreas, et al. "The neurophysiology and treatment of motion sickness." *Deutsches Ärzteblatt International* 115.41 (2018): 687.

Koleini, Navid, et al. "Ironing out mechanisms of iron homeostasis and disorders of iron deficiency." *The Journal of clinical investigation* 131.11 (2021).

Koplovitz, G., et al., 2019. Single domain 10 nm ferromagnetism imprinted on superparamagnetic nanoparticles using chiral molecules. Small 15, 1804557.

Kumar, K.S., et al., 2016. Long-range tunneling processes across ferritin-based junctions. Adv. Mater. 28, 1824–1830.

Labra-Muñoz, J.A., van der Zant, H.S.J., 2024. Ferritin single-electron transistor. J. Phys. Chem. B 128, 6387–6393.

Lauwers, M., et al., 2013. An iron-rich organelle in the cuticular plate of avian hair cells. Curr. Biol. 23, 924–929.

Lazzari, M., Bettini, S., Franceschini, V., 2013. Immunocytochemical characterization of olfactory ensheathing cells in fish. Brain Struct. Funct. 218, 539–549.

Lazzari, M., Bettini, S., Franceschini, V., 2014. Immunocytochemical characterisation of olfactory ensheathing cells of zebrafish. J. Anat. 224, 192–206.

Lekshmi, I.C., et al., 2011. Tunneling magnetoresistance with sign inversion in junctions based on iron oxide nanocrystal superlattices. ACS Nano 5, 1731–1738.

Lisowski, Clivia, et al. "Homing pigeon navigation relies on superparamagnetic macrophages under overcast conditions." *Science* 392.6801 (2026): 985-991.

Liu, L., et al., 2024. High iron in mouse olfactory ensheathing cells at the glia limitans in the olfactory bulb underlies MRI T2* hypointensity. Imaging Neurosci. 2, imag-2.

Mahmud, S., et al., 2026. A voltage-step method for detecting high-frequency transient current components in deep brain tissue: preliminary in vivo measurements in rats. bioRxiv preprint. [DOI to be added]

Malkemper, E.P., et al., 2019. No evidence for a magnetite-based magnetoreceptor in the lagena of pigeons. Curr. Biol. 29, R14–R15.

Mangia, S., Michaeli, S., Tuite, P., 2013. Magnetic resonance imaging (MRI) methods in Parkinson's disease. In: Magnetic Resonance Imaging in Movement Disorders: A Guide for Clinicians and Scientists, pp. 1–13.

Mietto, B.S., et al., 2021. Schwann cells provide iron to axonal mitochondria and its role in nerve regeneration. J. Neurosci. 41, 7300–7313.

Moldoveanu, V., Aldea, A., Manolescu, A., Niţă, M., 2000. Coulomb effects on the transport properties of quantum dots in a strong magnetic field. Phys. Rev. B 63, 045301. https://doi.org/10.1103/PhysRevB.63.045301

Morab, S., Sundaram, M.M., Pivrikas, A., 2023. Influence of traps and Lorentz force on charge transport in organic semiconductors. Materials 16, 4691.

Muñoz, P., et al., 2011. Iron mediates N-methyl-D-aspartate receptor-dependent stimulation of calcium-induced pathways and hippocampal synaptic plasticity. J. Biol. Chem. 286, 13382–13392.

Newton, K.C., Gill, A.B., Kajiura, S.M., 2019. Electroreception in marine fishes: chondrichthyans. J. Fish Biol. 95, 135–154.

Nimpf, S., et al., 2017. Subcellular analysis of pigeon hair cells implicates vesicular trafficking in cuticulosome formation and maintenance. eLife 6, e29959.

Nimpf, S., et al., 2019. A putative mechanism for magnetoreception by electromagnetic induction in the pigeon inner ear. Curr. Biol. 29, 4052–4059.

Nimpf, S., Keays, D.A., 2022. Myths in magnetosensation. iScience 25(6).

Petit, C.P., et al., 2026. Ferritin light-chain contributes to hair cells function and survival. Commun. Biol. [volume and article number to be added]

Reinert, A., et al., 2019. Iron concentrations in neurons and glial cells with estimates on ferritin concentrations. BMC Neurosci. 20, 25.

Rogge, M.C., Cavaliere, F., Sassetti, M., Haug, R.J., Kramer, B., 2006. Spin and negative differential conductance in the transport through a quantum dot in a magnetic field. Physica E 32, 442–445. https://doi.org/10.1016/j.physe.2005.12.086

Rourk, C., 2025. The bioelectric and biomagnetic properties of ferritin. Bioelectricity 7, 209–219.

Rourk, C., et al., 2021. Indication of strongly correlated electron transport and Mott insulator in disordered multilayer ferritin structures (DMFS). Materials 14, 4527.

Soares, M.P., Hamza, I., 2016. Macrophages and iron metabolism. Immunity 44, 492–504.

Soltis, J.A., et al., 2017. Electron mobility and trapping in ferrihydrite nanoparticles. ACS Earth Space Chem. 1, 216–226.

Takeuchi, H., 2024. Olfactory cilia, regulation and control of olfaction. Physiol. Rep. 12, e70057.

Treiber, C.D., et al., 2012. Clusters of iron-rich cells in the upper beak of pigeons are macrophages not magnetosensitive neurons. Nature 484, 367–370.

Wajnberg, E., et al., 2018. Ferritin from the haemolymph of adult ants: an extraction method for characterization and a ferromagnetic study. Eur. Biophys. J. 47, 641–653.

Walker, M.M., et al., 1997. Structure and function of the vertebrate magnetic sense. Nature 390, 371–376.

Watt, G.D., Frankel, R.B., Papaefthymiou, G.C., 1985. Reduction of mammalian ferritin. Proc. Natl. Acad. Sci. U.S.A. 82, 3640–3643.

Whitehead, D.L., et al., 2015. Morphology of the ampullae of Lorenzini in juvenile freshwater *Carcharhinus leucas*. J. Morphol. 276, 481–493.

Winklhofer, Michael, et al. "A macrophage-based magnetoreceptor is not tenable."

Wolszczak, M., Gajda, J., 2010. Iron release from ferritin induced by light and ionizing radiation. Res. Chem. Intermed. 36, 549–563.

Wosik, J., et al., 2018. Magnetic field changes macrophage phenotype. Biophys. J. 114, 2001–2013.

Yang, K.-H., Wang, X., Qin, C.-D., Wang, H.-Y., Cui, M., Dai, Y.-X., 2018. Magnetic field effects on transport through a strongly correlated dot coupled to Luttinger leads. J. Low Temp. Phys. 192, 286–298. https://doi.org/10.1007/s10909-018-1969-1

Zeng, H., et al., 2006. Magnetotransport of magnetite nanoparticle arrays. Phys. Rev. B 73, 020402(R).

Zhang, S.-N., Jiang, H., Liu, H., 2013. Numerical study of transport properties in topological insulator quantum dots under magnetic field. Mod. Phys. Lett. B 27, 1350104. https://doi.org/10.1142/S0217984913501042

Zhang, X., et al., 2018. Structural and functional components of the skate sensory organ ampullae of Lorenzini. ACS Chem. Biol. 13, 1677–1685.

Zhu, Q., et al., 2024. Magnetic monopole-like behavior in superparamagnetic nanoparticle coated with chiral molecules. Small 20, 2406631.

Zhuravel, D., Anchishkin, D.V., Hayn, R., Lombardo, P., Schäfer, S., 2019. Non-equilibrium electronic transport through a quantum dot with strong Coulomb repulsion in the presence of a magnetic field. J. Phys.: Condens. Matter (in press).

Zozoulenko, I.V., Maaø, F.A., Hauge, E.H., 1997. Coherent magnetotransport in confined arrays of antidots. III. Phys. Rev. B 56.

Figures and figure captions

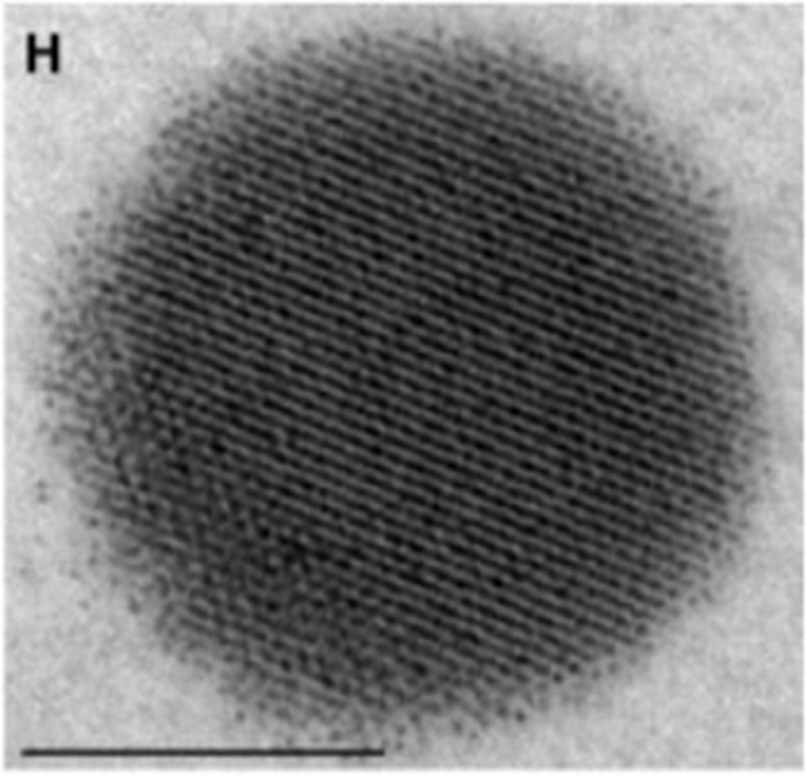

Fig. 1. Example of a ferritin-rich cuticulosome from an avian hair cell. Note the highly regular rows of ferritin particles. Reproduced from Nimpf et al. (2017) under a Creative Commons Attribution License.

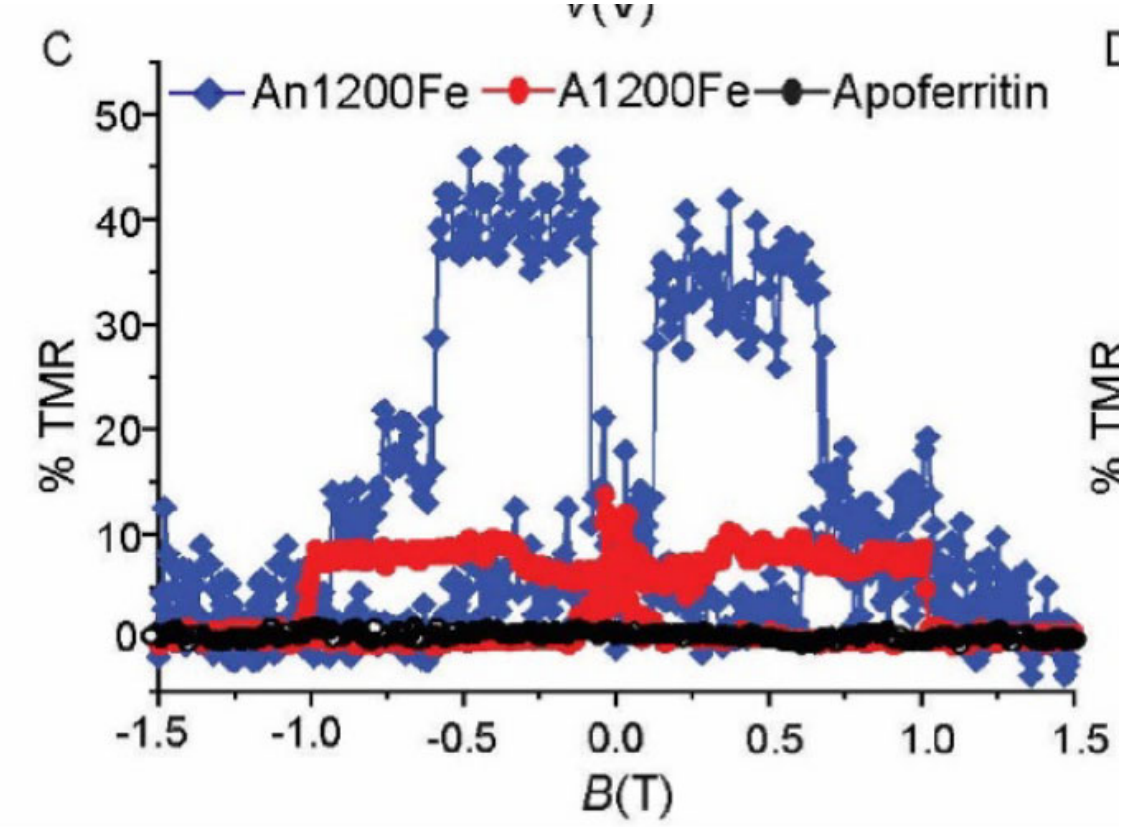

Fig. 2. Tunnel magnetoresistance of ferritin monolayers. An1200Fe is ferritin with 1,200 Fe^{3+} ions stored as iron oxides formed under anaerobic conditions; A1200Fe is ferritin with 1,200 Fe^{3+} ions stored as iron oxides formed under aerobic conditions. Compared with apoferritin, there is significant variability in the physical properties of ferritin even at low field strength. Reproduced from Karuppannan et al. (2021) under a Creative Commons Attribution License.

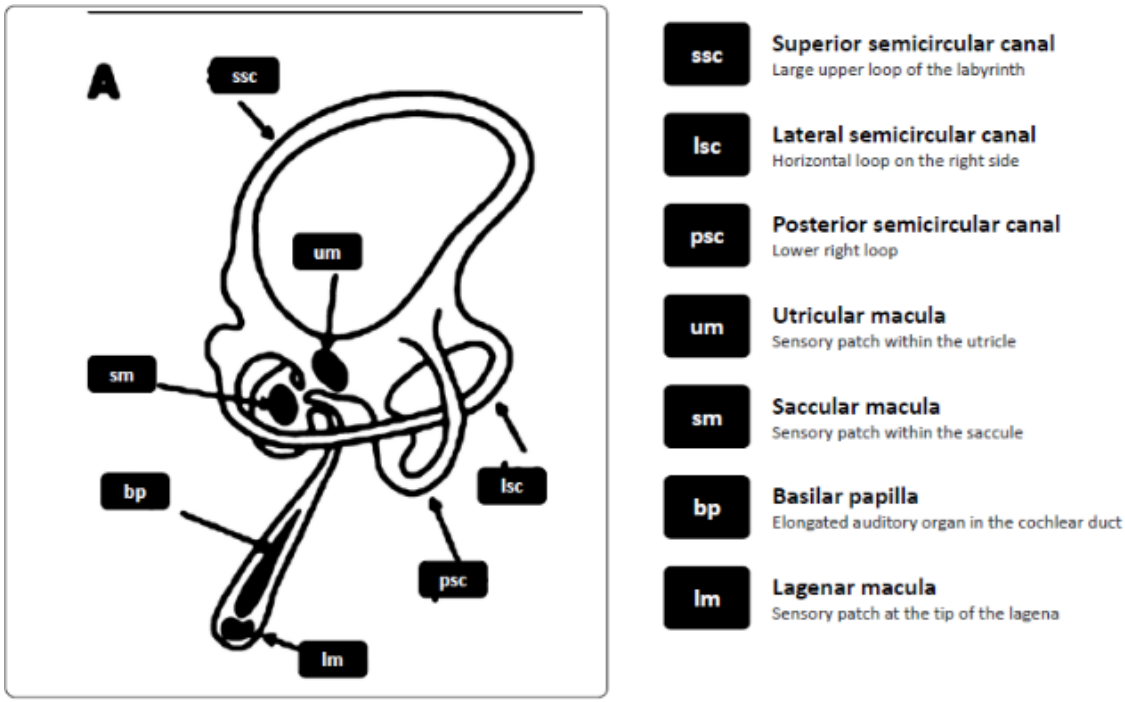

Fig. 3. Diagram of the avian auditory structure. ssc, superior semicircular canal; lsc, lateral semicircular canal; psc, posterior semicircular canal; um, utricular macula; sm, saccular macula; bp, basilar papilla; lm, lagenar macula.

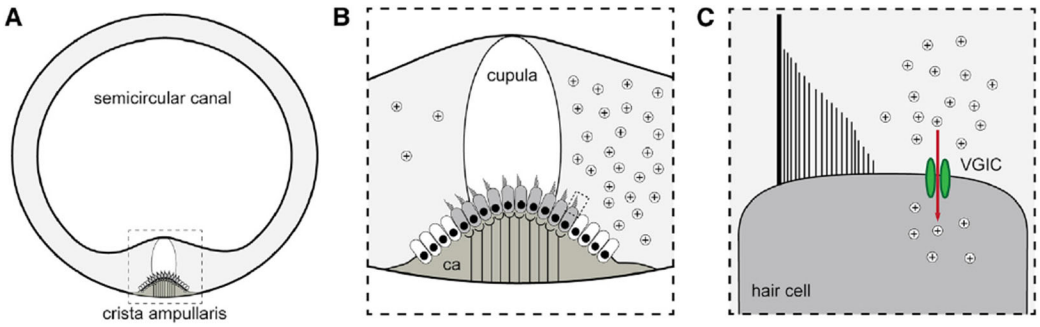

Fig. 4. Hair cells in the cupula and semicircular canal. Reproduced from Nimpf et al. (2019) under a CC BY license.

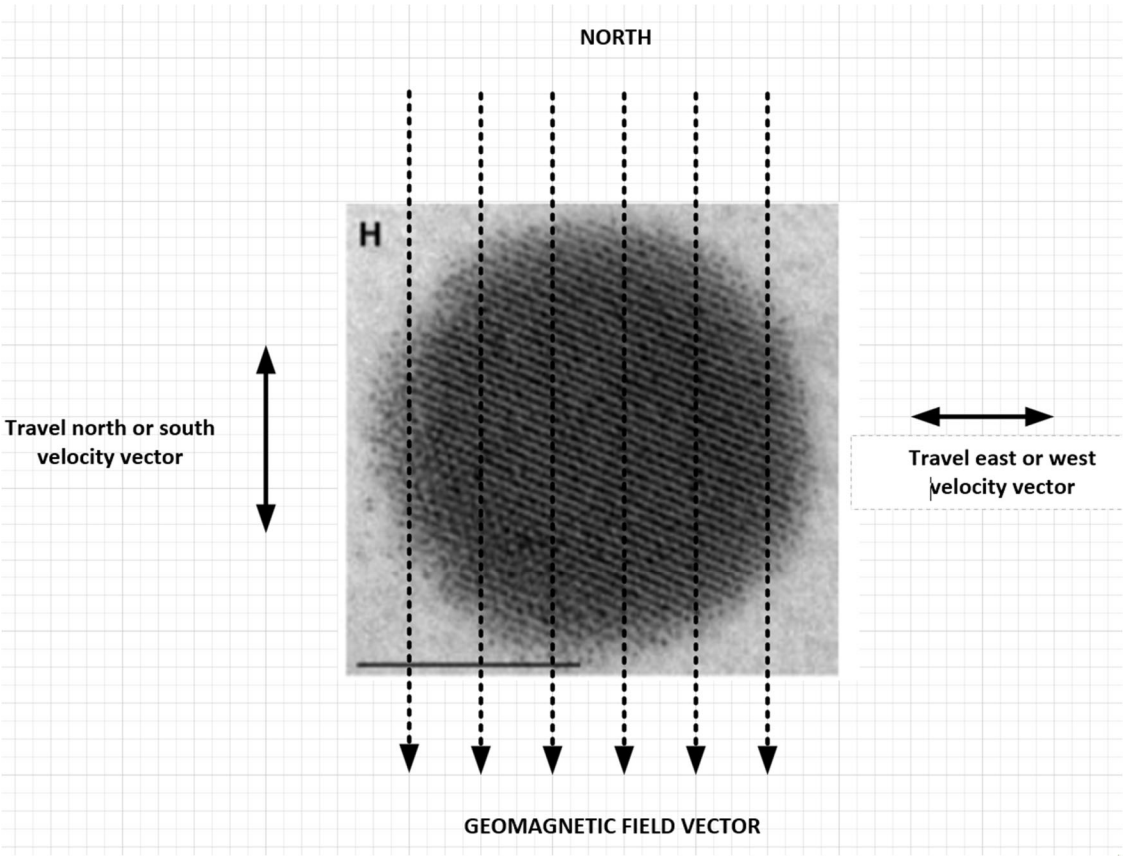

Fig. 5. Geomagnetic field vector and velocity vectors. The vectors are orthogonal for east or west travel but parallel for north or south travel.

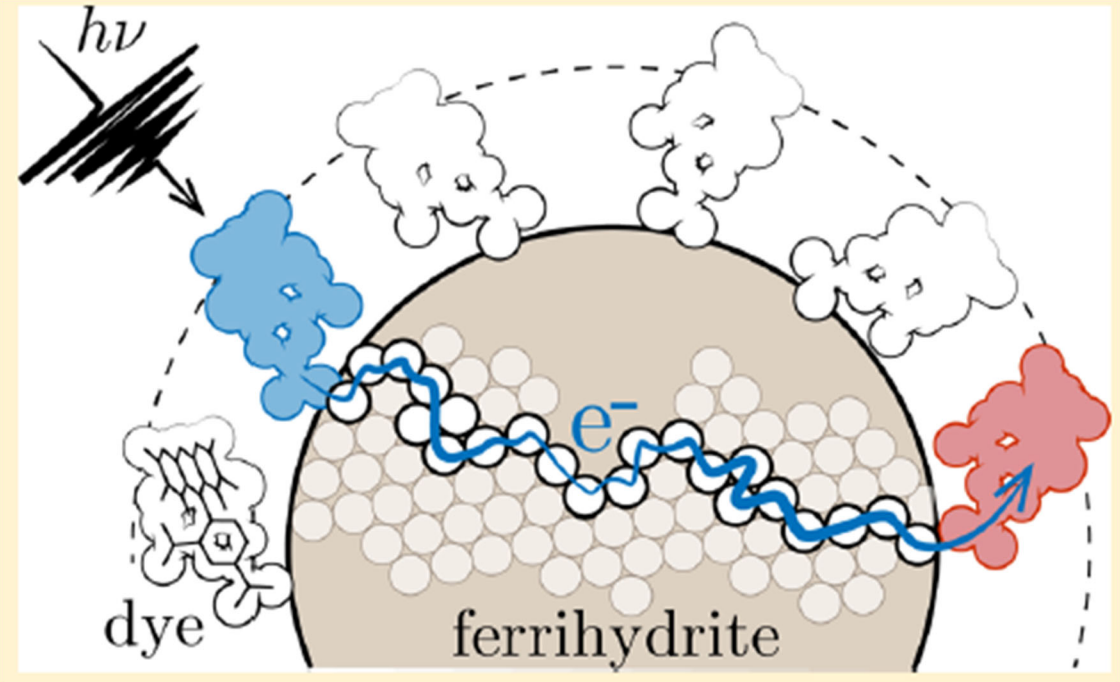

Fig. 6. Electron transport in ferrihydrite nanoparticles. Photon energy generates a free electron in a dye molecule adhered to the surface of an iron oxide nanoparticle; the electron then moves through the ferrihydrite nanoparticle by polaronic hopping. Long-time-scale retention of electrons that could not be explained by polaronic hopping indicates deep trap states persisting for 400 μs or longer. Image and data from Soltis et al. (2017).

Tables

Table 1. Electron transport characteristics of single ferritin particles compared with long-distance transport through three-dimensional ferritin arrays.

Layers	**Distance between electrodes**	**Applied voltage per core**	**Measured current (A/core)**	**Source**
1	12 nm (single core)	1 V	~1.13×10^{-20} to 10^{-25}	Kumar et al. (2016)
6	40 µm (~4,000 cores)	7.5×10^{-4} V	~4×10^{-13}	Bera et al. (2019)
5	80 µm (~8,000 cores)	3.75×10^{-4} V	~4×10^{-11}	Rourk et al. (2021)

Table 2. Fe^{2+} release dynamics of ferritin in vitro as a function of electrons stored in the core, after 20 min.

Electrons per Fe added	**Fe per ferritin after column**	**Fe lost**
0	2,346	0
0.25	2,285	15
0.50	2,115	185
0.75	1,900	400
1.00	1,850	450

Note: Data from Table 1 of Watt et al. (1985); “Fe lost” computed against the 2,300 Fe starting content.

Table 3. Estimates of Fe^{2+} release from electron dynamics in cuticulosome ferritin arrays.

Quantity	**Cochlear (545 nm)**	**Vestibular (365 nm)**
Ferritins (estimate)	~66,000	~20,000
Fe released at 450 per ferritin	~3.0×10^7 atoms (~4.9×10^{-17} mol)	~9×10^6 atoms (~1.5×10^{-17} mol)
Electrons required at 2,300 per ferritin	~1.5×10^8	~4.6×10^7
Concentration if dispersed in 1 pL	~49 μM	~15 μM

Note: Assumes 2,300 Fe^{3+} ions and release of 450 Fe^{2+} ions per ferritin particle (Watt et al., 1985), a packing fraction of 0.7, and a 1 pL cytoplasmic volume.

Table 4. Estimate of Fe^{2+} release required from ferritin in cuticulosomes to contribute to calcium signaling in astrocytes and neurons.

Calcium-signaling benchmark	**Fe atoms needed in 1 pL**	**Share of cochlear Watt-level release**	**Fe per ferritin**
0.5 μM (astrocyte EC_{50})	~3×10^5	~1%	~5
20 μM (neuronal RyR signaling)	~1.2×10^7	~40%	~180

Note: Benchmarks from Guan et al. (2021) (astrocytes) and Muñoz et al. (2011) (neurons); assumes a 1 pL cytoplasmic volume.

Table 5. Proposed tests of the hypothesis.

No.	Test	Setup	Prediction if hypothesis is correct
1	Conditioned aversion during transport	Move pigeons on a linear sled, rotating arm, or in a vehicle along E–W vs. N–S headings. Pair each heading with a distinct flavor or place, then measure flavor or place avoidance afterward (conditioned avoidance is a standard non-emetic proxy for motion sickness).	Aversion forms after E–W transport but not N–S.
2	Field manipulation during identical motion	Same motion protocol inside coils: (a) ambient field, (b) nulled field, (c) field rotated 90° so the "N–S" track becomes orthogonal, (d) field doubled or halved.	(a) and (c) produce aversion. (b) abolishes it. The effect scales with field strength, since the calculated force is proportional to B (60 μT vs. 24 μT examples). Test (c) also rules out cues tied to geography or the track itself.

No.	Test	Setup	Prediction if hypothesis is correct
3	Velocity dose–response	Vary speed.	Response rises with speed, because force is proportional to v. A response with no speed dependence argues against the mechanism.
4	Moving vs. stationary control	Rotate the field around a stationary bird at matched rates, and compare with moving the bird through a static field.	Only real movement through the field produces the effect. A response to field rotation alone points to induction or some other mechanism.
5	Neural activity mapping	Run a c-Fos/activity marker study after each condition. Look at the vestibular nuclei, where magnetically responsive neurons depend on an intact cochlear duct, and at emetic/motion-sickness centers.	More labeling after E–W/orthogonal exposure than after N–S/parallel or nulled-field exposure.

No.	Test	Setup	Prediction if hypothesis is correct
6	Ablation	Bilateral or unilateral removal of the cochlear duct/lagena, compared with sham surgery, then Tests 1–2.	Ablation abolishes the heading effect. This follows the existing dependency finding.
7	Iron, ROS, and calcium pathway blockade	Deliver locally into the inner ear, before exposure: an iron chelator, an antioxidant (to block Fenton chemistry), or ryanodine/IP_3 receptor blockers.	Each one attenuates the E–W effect, because the proposed chain is Fe^{2+} release, then ROS, then RyR/IP_3R calcium release. Standard anti-motion-sickness drugs should also reduce aversion if the endpoint really behaves like motion sickness.
8	Post-exposure tissue markers	Collect inner ear tissue right after exposure. Measure labile iron, lipid peroxidation or ROS markers, and cuticulosome ferritin iron content in hair cells.	More labile iron and ROS markers in hair cells after E–W exposure. Timing matters, because the LIP is expected to re-sequester Fe^{2+} quickly.

No.	Test	Setup	Prediction if hypothesis is correct
9	Free-flight heading choice	Release pigeons in a symmetric arena or flight tunnel with coil-controlled fields, and record the headings they choose.	Birds avoid flight axes orthogonal to the imposed horizontal field, consistent with the claim that the effect discourages E–W travel.
10	Ferritin ordering in cuticulosome	The alignment of ferritin in cuticulosomes should increase with age as a function of flight, such that free pigeons should achieve order faster than pigeons kept in aviaries.	Highly ordered linear arrays will form at younger ages in free pigeons compared to caged pigeons if travel through magnetic fields contributes to linearization of ferritin arrays.